J. Astrophys. Astr. (2018) 39:65
https://doi.org/10.1007/s12036-018-9556-z

Long-term ultraviolet variability of Seyfert galaxies

N. SUKANYA[1], C. S. STALIN[2], P. JOSEPH[2], S. RAKSHIT[2,3], D. PRAVEEN[4] and R. DAMLE[1,*]

[1]Department of Physics, Bangalore University, Bengaluru 560 056, India.
[2]Indian Institute of Astrophysics, Block II, Koramangala, Bengaluru 560 034, India.
[3]Department of Physics and Astronomy, Seoul National University, Seoul 08826, Republic of Korea.
[4]Physics Department, Amrita School of Engineering, Bengaluru 560 035, India.
*Corresponding author. E-mail: ramkrishnadamle@bub.ernet.in

MS received 29 September 2017; accepted 13 August 2018; published online 22 November 2018

Abstract. Flux variability is one of the defining characteristics of Seyfert galaxies, a class of active galactic nuclei (AGN). Although these variations are observed over a wide range of wavelengths, results on their flux variability characteristics in the ultraviolet (UV) band are very limited. We present here the long-term UV flux variability characteristics of a sample of fourteen Seyfert galaxies using data from the International Ultraviolet Explorer acquired between 1978 and 1995. We found that all the sources showed flux variations with no statistically significant differences in the amplitude of UV flux variation between shorter and longer wavelengths. Also, the flux variations between different near-UV (NUV, 1850−3300 Å) and far-UV (FUV, 1150−2000 Å) passbands in the rest frames of the objects are correlated with no time lag. The data show indications of (i) a mild negative correlation of UV variability with bolometric luminosity and (ii) weak positive correlation between UV variability and black hole mass. At FUV, about 50% of the sources show a strong correlation between spectral indices and flux variations with a hardening when brightening behaviour, while for the remaining sources the correlation is moderate. In NUV, the sources do show a harder spectrum when brighter, but the correlation is either weak or moderate.

Keywords. Active galaxies—Seyferts—variability.

1. Introduction

Active galactic nuclei (AGN) with observed bolometric luminosities of around $10^{11}-10^{14}\,L_{\odot}$, and that includes Seyfert galaxies amongst its class, are believed to be powered by accretion of matter onto supermassive black holes residing at the centres of galaxies (Lynden-Bell 1969; Rees 1984). According to the standard picture, accretion leads to the formation of an accretion disk that emits black body radiation. The observed ultraviolet (UV)/optical radiation in AGN is well represented by the superposition of several multi-temperature black body components (Frank *et al.* 2002) and the observed big blue bump (BBB) in AGN spectra is often attributed to the accretion disk.

AGN are known to show flux variations since their discovery and is now considered one of their defining characteristics (Wagner & Witzel 1995; Ulrich *et al.* 1997). Such flux variations are seen on a range of time scales from a fraction of hours to years over the complete electromagnetic spectrum from low-energy radio to high energy γ-rays (Wagner & Witzel 1995; Ulrich *et al.* 1997; Zhang & Feng 2017; Giveon *et al.* 1999). In spite of having a wealth of monitoring data on large samples of AGN with varying time resolutions through time domain surveys as well as dedicated monitoring programs, the physical mechanisms that cause AGN flux variations are still not well understood. Although different physical processes contribute to the emission at different wavebands, the UV–optical emission is believed to be emitted from an optically thick and geometrically thin accretion disk (Frank *et al.* 2002). Therefore, study of flux variations in the UV/optical bands can enable one to understand the processes happening in the accretion disk of AGN in particular in the non-blazar category of AGN.

Earlier efforts on the study of UV variations in AGN were by Paltani and Courvoisier (1994), who carried out a systematic analysis of the flux variations in the

UV of different classes of AGN using data from the international Ultraviolet Explorer (IUE) covering the period 1978–1991. Also, UV variability of blazars has been studied using IUE data (Edelson *et al.* 1991; Edelson 1992). According to their analysis, blazars show stronger variability at shorter wavelengths than at longer wavelengths. Subsequent to the work of Paltani and Courvoisier (1994), Welsh *et al.* (2011) carried out a systematic study of the UV variability of a large number of AGN using data from the Galaxy Evolution Explorer (GALEX) database. According to Welsh *et al.* (2011), the UV variability of quasars is much more than their optical fluctuations and among the UV bands, the variability observed in the far-UV (FUV; 1344−1786 Å) band is larger than the variability in the near-UV (NUV; 1771−2831 Å) band, which is also similar to that found by Paltani and Courvoisier (1994). The analysis of Paltani and Courvoisier (1994) failed to find any significant differences between the UV properties of radio-loud and radio-quiet quasars, prompting the authors to suggest that the UV emission from AGN is independent of the radio emission properties. Studies of optical flux variations in different categories of AGN indicate that blazars tend to show large amplitude and high duty cycles of variability within a night as compared to other radio-loud and radio-quiet AGN (Stalin *et al.* 2004). On year-like time scales, among Seyfert galaxies in the optical band, radio-loud sources are more variable than their radio-quiet counterparts (Rakshit & Stalin 2017).

Short-time-scale UV flux variations of the order of 1000 to 10000 s were found in the Seyfert 1 galaxy NGC 7469 by Welsh *et al.* (1998), using the Faint Object Spectrograph on the Hubble Space Telescope as well as Fairall 9 (Lohfink *et al.* 2014). Most of the studies on the UV flux variability of AGN (Sakata *et al.* 2011; Paltani & Courvoisier 1994) either using spectroscopy or broadband photometry indicate that the UV flux variability characteristics of AGN can be well described by accretion disk models. Vanden Berk *et al.* (2004), based on two epochs of observations on a large number of quasars, found a spectral hardening of the UV continuum emission with increasing flux values. Similar results were also found by Wilhite *et al.* (2005) using spectroscopic observations. Paltani and Walter (1996), using IUE observations, observed that the spectra of Seyfert galaxies vary with time and they become flatter when the source brightens. To explain the observations, they proposed a two component model wherein the UV flux variations consist of a variable component with a constant spectral shape and a non-variable component from the small blue bump (SBB). Also, there are reports that claim the constancy of UV spectral shape during flux variations of AGN (Alloin *et al.* 1995; Rodriguez-Pascual *et al.* 1997). As we have limited studies on the UV flux variability characteristics of AGN both in the long term as well as short term, it is of great importance to expand the studies on the already known UV flux variability nature of AGN to a larger sample of sources, and having data for a longer duration of time than that analysed earlier by Paltani and Walter (1996). Towards this, we have carried out a statistical analysis of the UV variability of a sample of Seyfert galaxies, a category of AGN for which sufficient data is available and focussed mainly on the FUV (1150–2000 Å) and NUV (1850−3200 Å) flux variations.

2. Sample and data

Our sample of Seyfert 1 galaxies was taken from Dunn *et al.* (2006) who have provided continuum light curves in different wavebands for a sample of 175 Seyfert galaxies as part of the Program in Extra Galactic Astronomy (PEGA).[1] The data in this compilation were taken from the observations carried by IUE between the period 1978 and 1995. In this database, Dunn *et al.* (2006) have provided continuum flux measurements at three line-free regions in the spectra of each of the Seyfert galaxies. In IUE spectra, the NUV and FUV cover the wavelength regions 1850−3200 Å and 1150–2000 Å respectively. For most of the sources, flux measurements are available in three NUV passbands (2200, 2400 and 2740 Å) with bin sizes of 50, 60 and 30 Å and three FUV passbands (1355, 1720 and 1810 Å) with bin sizes of 30, 30 and 50 Å. For this study, we have downloaded the light curves for all the Seyfert galaxies that are available in the PEGA database and we applied the following conditions to select the light curves for further analysis:

1. The sources must have data from the two cameras of IUE, namely, the short-wavelength prime (SWP) and long-wavelength prime (LWP).
2. The total number of points (that includes all the three continuum passbands in FUV and NUV) must be larger than 50.

The above two conditions led us to a final sample of 14 Seyfert galaxies spanning the redshift range $0.002 < z < 0.07$. Of the 14 selected Seyfert galaxies, one galaxy (NGC 1068) belongs to the Seyfert 2 category (having narrow permitted and forbidden lines),

[1] http://www.astro.gsu.edu/PEGA/IUE.

while the remaining 13 sources belong to the Seyfert 1 category with broad permitted lines and narrow forbidden lines. The details of the objects selected for this study are given in Table 1. In this table, the total in column 7 refers to the total number of photometric points for a source in all the six passbands together. The entries against λ_1, λ_2 and λ_3 in SWP and LWP columns refer to the central wavelength used for the photometry and N_{NUV} and N_{FUV} give the number of points in each of the NUV and FUV passbands.

The observed flux values in all the six passbands were corrected for galactic extinction using the A_V values taken from NED,[2] which uses Schlafly and Finkbeiner (2011) and the extinction law evaluated in the UV range using the formalism given by Cardelli *et al.* (1989). The galactic extinction corrected flux values were then subjected to further analysis. We note here that the measured flux values were not corrected for extinction due to the host galaxies of the sources. The light curves in all the FUV and NUV passbands for the sources are given in Fig. 1 through Fig. 5. In these figures, the quoted wavelengths are in the observed frame of the sources. The present sample analysed here has some overlap with that reported by Paltani and Walter (1996). The sample analysed by Paltani and Walter (1996) has 15 sources that includes Seyfert galaxies, radio-loud as well as radio-quiet quasars. Their analysis was based on IUE data collected up to 1991. Our sample analysed here contains 14 Seyfert galaxies using data from IUE upto 1995. Though there are 10 sources in common to the sample reported here and that of Paltani and Walter (1996), the data analysed here is more extended in terms of the number of epochs and the total duration (1978–1995) as compared to Paltani and Walter (1996), who have analysed data from IUE until 1991.

2.1 *Flux variability*

For all the 14 sources selected based on the criteria outlined above, we carried out analysis to characterise their variability. This was done by calculating their normalized excess variance defined in Vaughan *et al.* (2003) as

$$F_{var} = \sqrt{\frac{S^2 - \overline{\sigma_{err}^2}}{\overline{x}^2}} \tag{1}$$

where S^2 and σ_{err}^2 are the sample variance and average error defined as

$$S^2 = \frac{1}{N-1}\sum_i (x_i - \overline{x})^2 \tag{2}$$

$$\overline{\sigma_{err}^2} = \frac{1}{N}\sum_{i=1}^{N} \sigma_{err,i}^2 \tag{3}$$

The error in F_{var} was calculated again using Vaughan *et al.* (2003) and is defined as

$$\sigma_{F_{var}} = \sqrt{\left(\sqrt{\frac{1}{2N}}\frac{\overline{\sigma_{err}^2}}{\overline{x}^2 F_{var}}\right)^2 + \left(\sqrt{\frac{\overline{\sigma_{err}^2}}{N}}\frac{1}{\overline{x}}\right)^2} \tag{4}$$

The majority of the sources in our sample have overlapping coverage in FUV and NUV passbands except for five sources, namely, 3C 120, 3C 390.3, NGC 3516, NGC 7469 and NGC 4051. This is evident in the light curves of these sources shown in Figs. 1, 3 and 5. Because of this, for calculating F_{var}, we have considered only those duration of the light curves that have overlapping coverage in both FUV and NUV passbands. The calculated F_{var} values for all the sources in each of the six continuum passbands are given in Table 2. A source is considered variable if its F_{var} is greater than zero, and it is significant at the one sigma level. In all instances in our sample, F_{var} is many times greater than their associated errors except in four cases where it is less than three times their associated errors. Among these four too, in two cases F_{var} is more than two times their associated errors and in the remaining two cases it is between one and two sigma. We therefore argue that all the sources in the sample analysed here are highly variable in all the six passbands, except in four instances where the variability is less significant. The mean F_{var} values in all the six passbands for all the sources studied here is shown in Table 3. There is an indication that the variations at the shorter wavelengths are larger than those at the longer wavelengths, but the larger error bars preclude us to draw any firm conclusion on the differences in variability between different wavelengths. Clubbing the F_{var} values in the three SWP passbands together as SWP and the three LWP passbands together as LWP, we obtained simple average values of F_{var} as 0.392 ± 0.196 and 0.293 ± 0.152 for SWP and LWP respectively. The total number of F_{var} values are thus 42, in each of the SWP and LWP passbands. The distributions of F_{var} for SWP and LWP and their cumulative distributions are given in Figs. 6 and 7 respectively. The average value of F_{var} is larger in SWP than in LWP, however, as the error bars are larger we carried out a two sample KS test. The null hypothesis that was tested was that the two independent F_{var} values pertaining to SWP and LWP were drawn from the

[2] ned.ipac.caltech.edu.

Table 1. Details of the objects studied for variability. The M_{BH} values are in solar units, and were taken from the data base of Bentz and Katz (2015) except for the sources NGC 1068 and Mrk 478 where it was taken from Greenhill and Gwinn (1997) and Wang *et al.* (2001) respectively.

Name	RA(2000)	Dec (2000)	Redshift	log (M_{BH})	L_{bol} (erg/sec)	N_{Total}	SWP				LWP			
							λ_1	λ_2	λ_3	N_{FUV}	λ_1	λ_2	λ_3	N_{NUV}
Fairall 9	01:23:45.8	−58:48:20.5	0.047	8.299	44.78	693	1418	1800	1895	156	2303	2512	2868	75
NGC 1068	02:42:40.7	−00:00:47.8	0.004	7.176	44.60	75	1360	1726	1816	14	2208	2409	2750	11
3C 120	04:33:11.1	+05:21:15.6	0.033	7.745	43.98	186	1399	1776	1869	42	2272	2479	2830	20
Akn 120	05:16:11.4	−00:08:59.4	0.032	8.068	44.40	177	1398	1775	1868	36	2271	2471	2828	23
NGC 3516	11:06:47.5	+72:34:06.9	0.009	7.395	43.89	330	1366	1735	1826	85	2219	2421	2764	25
NGC 3783	11:39:01.8	−37:44:18.7	0.010	7.371	43.57	834	1368	1736	1827	164	2221	2423	2726	114
NGC 4051	12:03:09.6	+44:31:52.8	0.002	6.130	42.38	117	1358	1724	1814	30	2205	2405	2746	9
NGC 4151	12:10:32.6	+39:24:20.6	0.003	7.555	43.30	2904	1359	1725	1816	542	2207	2407	2749	426
NGC 4593	12:39:39.4	−05:20:39.3	0.009	6.882	43.45	138	1367	1735	1826	29	2219	2421	2764	17
NGC 5548	14:17:59.5	+25:08:12.4	0.017	7.718	43.92	1104	1378	1749	1841	214	2237	2441	2787	154
Mrk 478	14:42:07.5	+35:26:22.9	0.079	7.330	44.95	117	1462	1855	1953	19	2373	2589	2956	20
3C 390.3	18:42:09.0	+79:46:17.1	0.056	8.638	44.32	330	1431	1816	1911	94	2323	2534	2893	16
Mrk 509	20:44:09.7	−10:43:04.5	0.034	8.049	44.78	288	1401	1779	1872	55	2275	2482	2834	41
NGC 7469	23:03:15.6	+08:52:26.4	0.016	6.956	44.42	750	1377	1748	1839	236	2235	2439	2784	14

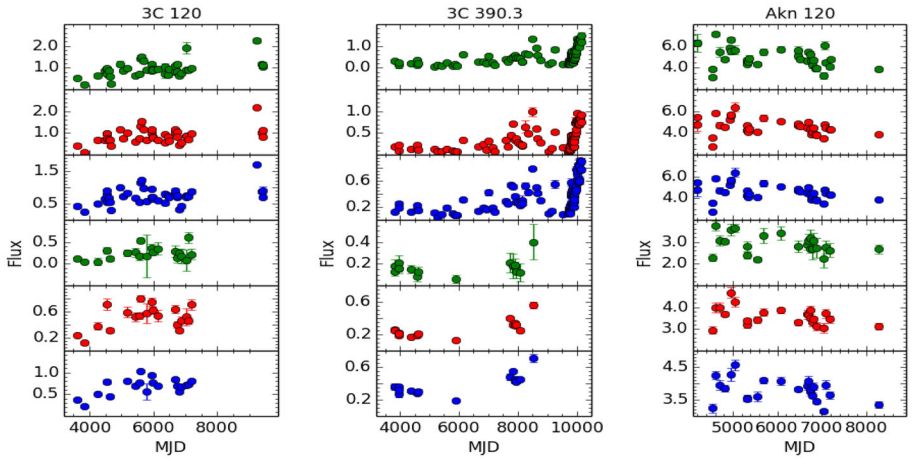

Figure 1. FUV and NUV light curves. The top three panels are for the FUV bands and the light curves in the bottom three panels are for NUV bands. For 3C 120, from top to bottom the wavelength of the light curves are 1399 Å, 1776 Å, 1869 Å, 2272 Å, 2479 Å and 2830 Å. For 3C 390.3, the wavelength of the light curves from top to bottom are 1431 Å, 1816 Å, 1911 Å, 2323 Å, 2534 Å and 2893 Å. For Akn 120, the light curves shown from top to bottom are in wavelengths of 1390 Å, 1775 Å, 1868 Å, 2271 Å, 2477 Å and 2828 Å.

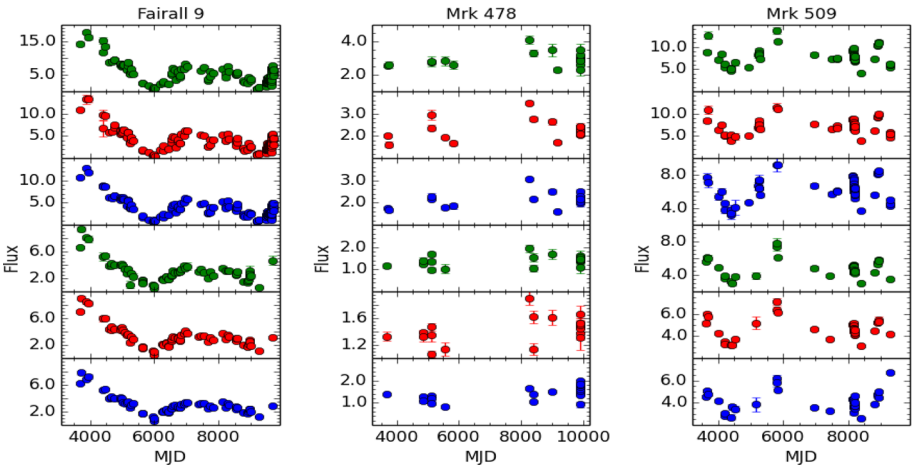

Figure 2. Light curves in increasing order of wavelengths from top to bottom for Fairall 9 (left), Mrk 478 (middle) and Mrk 509 (right). For Fairall 9, the wavelengths are 1418 Å, 1800 Å, 1895 Å, 2303 Å, 2512 Å and 2868 AA. For Mrk 478, the light curves from top to bottom have wavelengths of 1462 Å, 1855 Å, 1953 Å, 2373 Å, 2589 Å and 2956 Å. For Mrk 509, from the top to the bottom panels, the light curves have the wavelengths of 1401 Å, 1779 Å, 1872 Å, 2275 Å, 2482 Å and 2834 Å.

same distribution. This null hypothesis was accepted, as D was lesser than the critical value of D (D_{crit}). We obtained values of 0.286 and 0.356 for D and D_{crit} respectively for a significance level of 0.01. This statistically points to no difference in the F_{var} values between SWP and LWP bands. Available studies do indicate that in UV, AGN show wavelength-dependent variability, with shorter wavelengths showing large amplitude of variability compared to the longer wavelengths (Sakata *et al.* 2011; Vanden Berk *et al.* 2004; Welsh *et al.* 2011). Data analysed here do indicate that variations at the shorter wavelengths are larger than that at longer wavelengths; however, due to the quality of the data, the error bars are too large to draw any conclusion on variation of amplitude of variability with wavelength.

3. Correlation between variability and other physical properties

3.1 F_{var} and L_{bol}

To find the presence of any correlation between F_{var} and bolometric luminosity (L_{bol}), we plotted in Fig. 8 the variation of F_{var} with L_{bol}. The F_{var} values used in this correlation analysis is for the NUV band for the

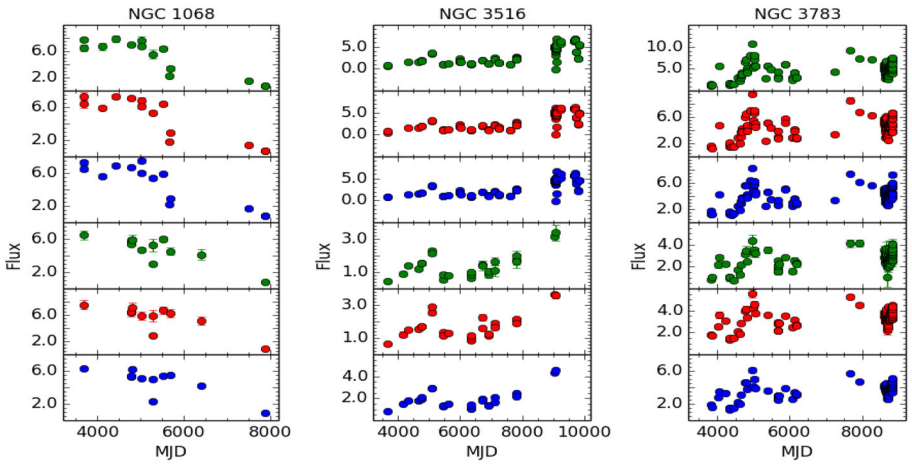

Figure 3. Light curves in FUV and NUV bands for the sources NGC 1068 (left), NGC 3516 (middle) and NGC 3783 (right). For NGC 1068 the light curves from the top to the bottom panels are at wavelengths of 1360 Å, 1726 Å, 1816 Å, 2208 Å, 2409 Å and 2750 Å. For NGC 3516 the light curves are at increasing order of wavelengths from top to bottom and have wavelength values of 1366 Å, 1735 Å, 1826 Å, 2219 Å, 2421 Å and 2764 Å. For NGC 3783, the light curves from top to bottom panels have wavelengths of 1368 Å, 1736 Å, 1827 Å, 2221 Å, 2423 Å and 2766 Å.

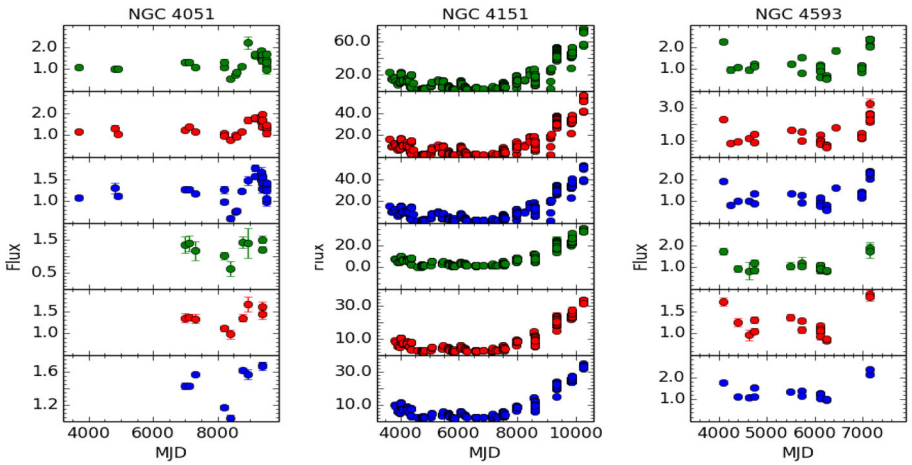

Figure 4. Light curves in FUV and NUV bands for the sources NGC 4051, NGC 4151 and NGC 4593. For NGC 4051, the light curves in increasing order of wavelength from top to bottom are at wavelengths of 1358 Å, 1724 Å, 1814 Å, 2205 Å, 2405 Å and 2746 Å. For NGC 4151, the light curves are at 1359 Å, 1725 Å, 1816 Å, 2207 Å, 2407 Å and 2749 Å from the top to the bottom panels. For NGC 4593, the shown light curves from top to bottom are for wavelengths of 1367 Å, 1735 Å, 1826 Å, 2219 Å, 2421 Å and 2764 Å.

passband 2806 ± 64 Å. We used the relation $L_{bol} = 13.2 \times L_V$ given by Elvis *et al.* (1994). Here, L_V is the luminosity in the V-band which was derived using the V-band magnitude of the sources taken from SIMBAD,[3] the zero-points taken from Bessel (1979) and the luminosity distance taken from NED.[4] Using all the F_{var} values, we found indication of no correlation between F_{var} and L_{bol} with a low correlation coefficient of −0.08 and a probability of no correlation of $P = 0.79$. This trend for no correlation between F_{var} and L_{bol} is due to one low luminosity source NGC 4051. Neglecting this source and doing a linear least squares fit to the data gave evidence for a mild negative correlation between F_{var} and L_{bol}. The linear least square fit is shown as a dashed line in Fig. 8. Correlation analysis indicates a mild negative correlation with a correlation coefficient of −0.39 with a probability of no correlation of $P = 0.19$. This is in agreement with what is known in literature. Using IUE data, Paltani and Courvoisier (1997) found an anti-correlation between quasar variability and luminosity with high-luminosity

[3] http://simbad.u-strasbg.fr/simbad/.

[4] http://www.astro.ucla.edu/~wright/CosmoCalc.html.

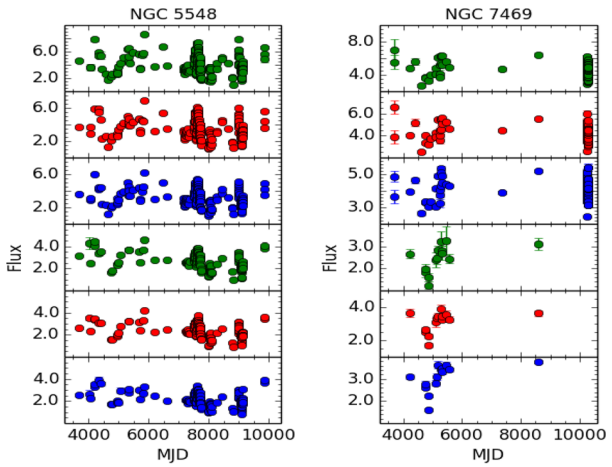

Figure 5. FUV and NUV light curves for the sources NGC 5548 and NGC 7469. For NGC 5548, the wavelengths of the light curves from top to bottom are 1378 Å, 1749 Å, 1841 Å, 2237 Å, 2441 Å and 2787 Å. For NGC 7469 the light curves shown from top to bottom have wavelengths of 1377 Å, 1748 Å, 1839 Å, 2235 Å, 2439 Å and 2784 Å.

quasars showing low-amplitude of variability. This anti-correlation is also seen in the optical bands (Vanden Berk *et al.* 2004; Meusinge & Weiss 2013). Analysing large sample of quasars for UV variability using data from GALEX, Welsh *et al.* (2011) found two different correlations between variability and luminosity. For time lags greater than 100 days, variability is negatively correlated with luminosity, while for time lags lesser than 100 days, variability is positively correlated with luminosity. The data analysed here too reveal a negative correlation between UV variability and luminosity. However, quality UV data (with similar time resolution and uniform coverage in both FUV and NUV) on a larger sample of sources are needed to firmly establish this finding.

3.2 F_{var} and M_{BH}

Correlation between optical variability and black hole (BH) mass has been widely studied in the optical region with no clear consensus. From an analysis of the long term optical variability of quasars, Wold *et al.* (2007) found a correlation between variability and BH mass with sources with large BH mass showing larger amplitude of variability. Such a correlation was also noticed by Wilhite *et al.* (2008); however, Meusinge and Weiss (2013) and Zuo *et al.* (2012) could not find any correlation between optical variability and BH mass. From the data set analysed here, we looked for the existence of any correlation between UV variability and BH mass. In Fig. 9 we show the correlation between F_{var} and M_{BH} where we found hint for a positive correlation between F_{var} and M_{BH}. Correlation analysis gave a Pearson's rank correlation coefficient of 0.18 with probability for no correlation being 0.54. The F_{var} values used in this correlation analysis too is in NUV for the passband 2806 ± 64 Å.

4. Spectral variability

To know the spectral variability nature of the sources studied here, we examined the change in the spectral index relative to the flux of the sources. The optical to UV continuum slope of an AGN can be well represented as a power law, $F_\nu \propto \nu^{-\alpha}$, where F_ν is the observed flux density and α is the spectral index. For each of the sources studied here, we have observations in six UV passbands. We therefore calculated the spectral index by fitting a power law of the form

$$F_\lambda \propto \lambda^{\alpha-2} \tag{5}$$

For NUV, α was determined using the above power law fit to three measurements and for FUV again three measurements were used to derive α. The variation of α thus deduced against the flux of the sources in both SWP and LWP are shown in Figs. 10 and 11 respectively. For SWP, we selected the shortest wavelength of three, and for LWP, we selected the shortest wavelength of the three observations. This was only for the purpose of defining the flux values. For the analysis of correlation between α and flux, we considered only those points where the error in α and flux values are lower than the associated values of α and fluxes. The data were fit with a straight line by (i) assigning equal weight to all the points and (ii) taking into account the errors in both α and flux values. The un-weighted linear least squares fits are shown by dashed lines in Figs. 10 and 11, while the weighted linear least squares fits are shown by solid lines. From weighted linear least squares fit to the data we find that, for most of the sources, their spectra do not show any significant changes during the flux variations; however, for few sources, we found clear evidence of a hardening of the spectra with increase in flux. For some sources, we see structures in the variation of α with flux. The spectrum is found to harden with increasing flux; however, limited to certain moderate flux values, beyond which the spectrum is nearly steady showing no change with flux. This is seen in the sources NGC 3783, NGC 4151, NGC 4593 and Fairall 9 in SWP. In LWP, this is evident in the sources NGC 4151 and Fairall 9. The results of the linear least squares fit to the variation

Table 2. Results of the analysis of variability. The entries in columns 2, 3 and 4 are for the FUV bands, while the entries in columns 5,6 and 7 are for the NUV bands. Columns 8 and 9 give the mean α in SWP and LWP, and the last column gives the mean α estimated using IUE data covering the range of 1150 –3200 Å and taken from Paltani and Walter (1996).

Name	$F_{var} \pm \sigma_{F_{var}}$						$\overline{\alpha}$(SWP)	$\overline{\alpha}$(LWP)	$\overline{\alpha}$
	SWP			LWP					
	λ_1	λ_2	λ_3	λ_1	λ_2	λ_3			
Fairall 9	0.586 ± 0.012	0.574 ± 0.012	0.562 ± 0.006	0.515 ± 0.022	0.499 ± 0.012	0.440 ± 0.009	0.92 ± 0.04	1.68 ± 0.05	0.9
NGC 1068	0.529 ± 0.052	0.548 ± 0.036	0.522 ± 0.028	0.335 ± 0.073	0.339 ± 0.086	0.351 ± 0.022	1.68 ± 0.10	1.28 ± 0.15	—
3C 120	0.321 ± 0.058	0.327 ± 0.030	0.297 ± 0.026	0.414 ± 0.157	0.336 ± 0.052	0.282 ± 0.017	0.80 ± 0.09	2.46 ± 0.20	1.9
Akn 120	0.174 ± 0.035	0.154 ± 0.022	0.154 ± 0.022	0.109 ± 0.057	0.104 ± 0.029	0.086 ± 0.017	1.41 ± 0.04	1.60 ± 0.07	1.5
NGC 3516	0.600 ± 0.013	0.596 ± 0.012	0.590 ± 0.008	0.495 ± 0.044	0.435 ± 0.019	0.461 ± 0.011	1.75 ± 0.03	2.81 ± 0.10	2.2
NGC 3783	0.305 ± 0.013	0.278 ± 0.010	0.269 ± 0.008	0.225 ± 0.035	0.217 ± 0.014	0.221 ± 0.007	1.15 ± 0.02	1.67 ± 0.04	1.5
NGC 4051	0.240 ± 0.021	0.215 ± 0.016	0.206 ± 0.012	0.109 ± 0.076	0.137 ± 0.031	0.151 ± 0.011	1.91 ± 0.11	2.52 ± 0.13	—
NGC 4151	0.749 ± 0.011	0.728 ± 0.008	0.708 ± 0.006	0.681 ± 0.030	0.629 ± 0.016	0.650 ± 0.006	0.99 ± 0.02	2.25 ± 0.03	1.2
NGC 4593	0.440 ± 0.016	0.462 ± 0.018	0.407 ± 0.011	0.246 ± 0.048	0.254 ± 0.019	0.284 ± 0.012	2.03 ± 0.08	2.53 ± 0.07	2.0
NGC 5548	0.362 ± 0.008	0.337 ± 0.006	0.315 ± 0.004	0.253 ± 0.008	0.262 ± 0.004	0.271 ± 0.006	1.22 ± 0.02	1.06 ± 0.04	1.3
Mrk 478	0.119 ± 0.039	0.196 ± 0.018	0.153 ± 0.016	0.134 ± 0.032	0.119 ± 0.019	0.226 ± 0.012	1.00 ± 0.13	1.88 ± 0.08	—
3C 390.3	0.712 ± 0.027	0.780 ± 0.018	0.645 ± 0.014	0.144 ± 0.056	0.367 ± 0.016	0.309 ± 0.015	1.57 ± 0.15	4.43 ± 0.18	—
Mrk 509	0.234 ± 0.024	0.230 ± 0.027	0.226 ± 0.021	0.209 ± 0.024	0.183 ± 0.016	0.207 ± 0.018	1.13 ± 0.04	0.80 ± 0.04	1.2
NGC 7469	0.215 ± 0.047	0.204 ± 0.029	0.183 ± 0.020	0.213 ± 0.068	0.189 ± 0.037	0.195 ± 0.021	1.31 ± 0.02	1.73 ± 0.16	1.4

Table 3. Average F_{var} values for the different wavelength bands.

Mean wavelength	Mean F_{var}
1389 ± 30	0.399 ± 0.198
1762 ± 38	0.402 ± 0.203
1855 ± 40	0.374 ± 0.188
2255 ± 49	0.292 ± 0.168
2460 ± 53	0.291 ± 0.148
2806 ± 64	0.295 ± 0.139

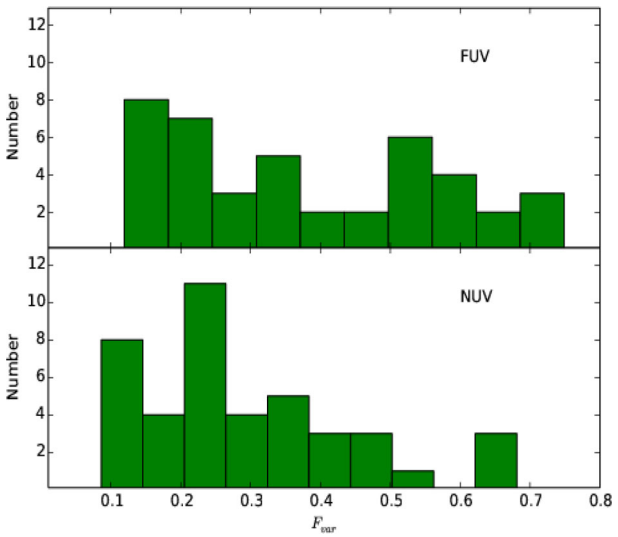

Figure 6. Distribution of F_{var} values for the sources studied here in FUV (top panel) and NUV (bottom panel) bands.

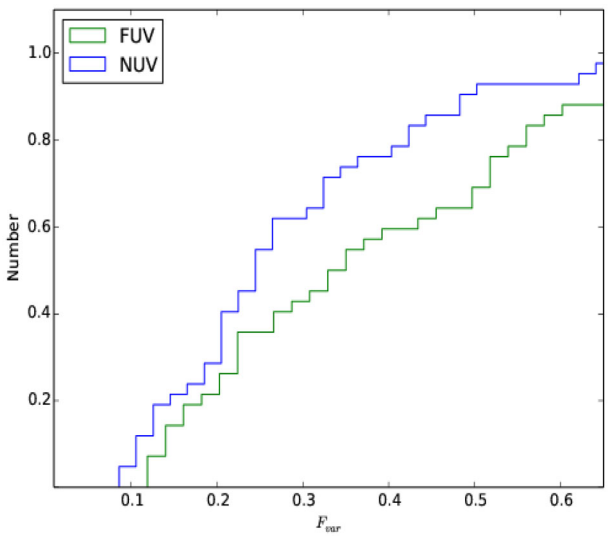

Figure 7. Cumulative distribution of the values of F_{var} in FUV (in green) and NUV (in blue) bands.

in α with flux is shown in Table 4. In FUV about 50% of the sources showed a harder when brighter trend. The

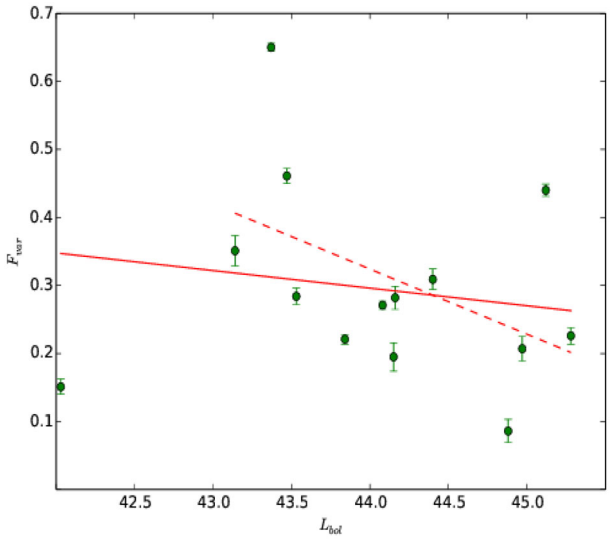

Figure 8. Variation of F_{var} with bolometric luminosity. Linear least squares fit to the data are shown for the complete data (solid line) and for the data set excluding the lowest luminosity source in our sample (dashed line).

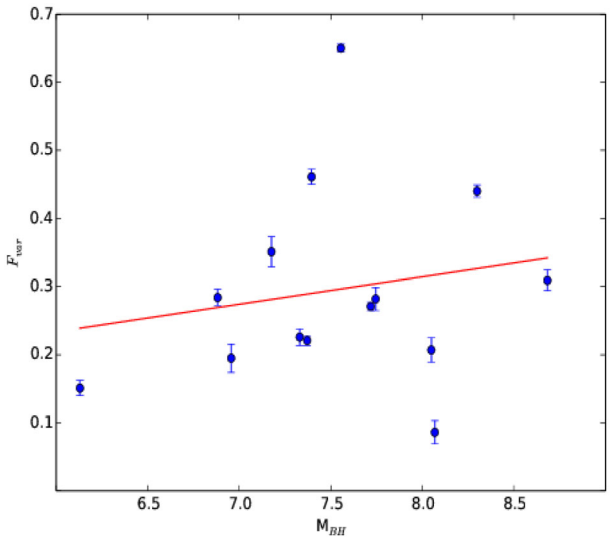

Figure 9. Plot of F_{var} against black hole mass. The solid line is the linear least squares fit to the data.

remaining sources too showed a harder when brighter behaviour but the correlation is moderate. The weighted and un-weighted linear least squares fit show similar trend for most of the sources, with the largest mismatch seen in Mrk 478. In the NUV band there is moderate correlation between α and the flux with a trend for a harder when brighter behaviour. Here too, large discrepancy between weighted and un-weighted linear least squares fits is seen in sources such as Mrk 478, NGC 4593 and 3C 390.3. These results to a large extent agree with the analysis of the UV continuum emission

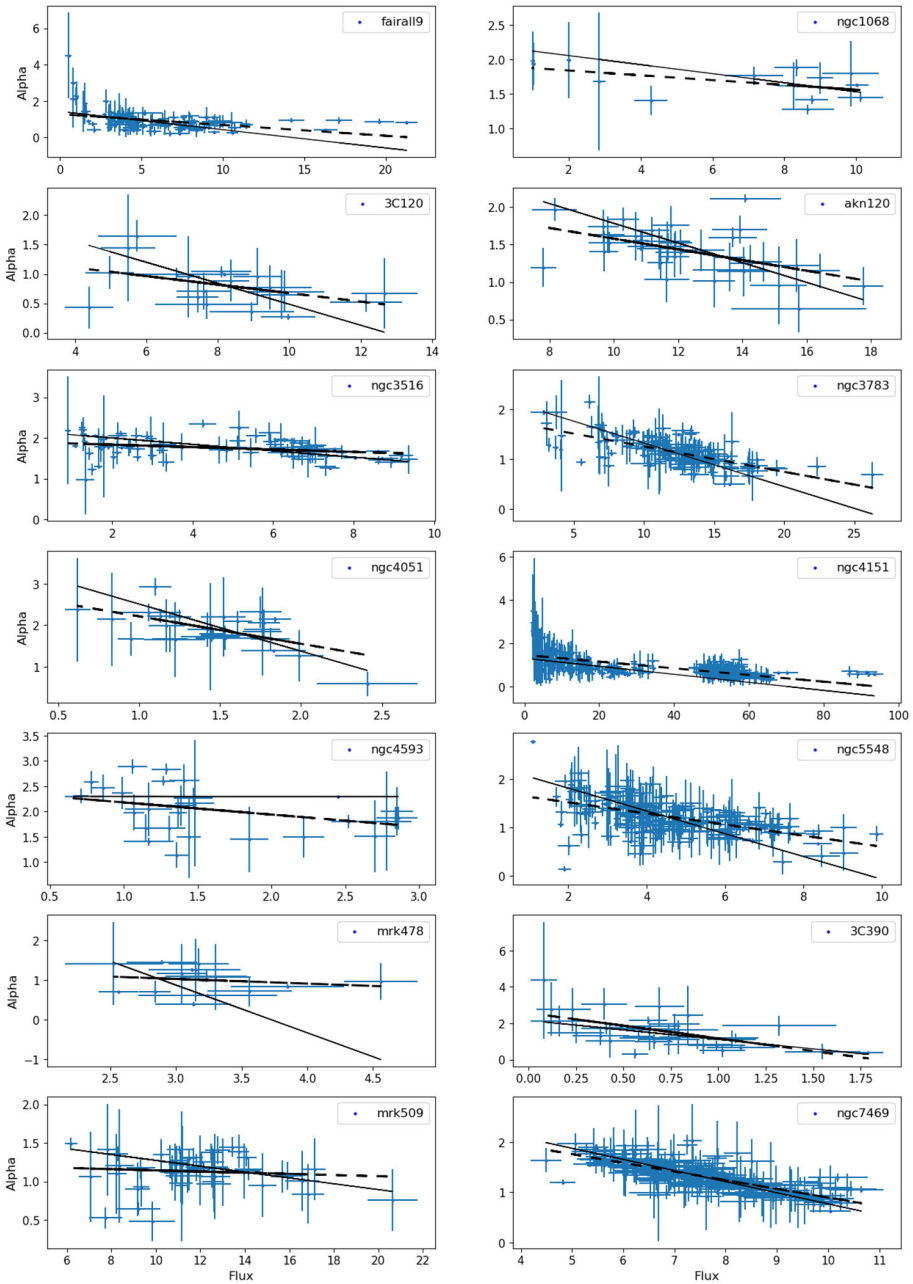

Figure 10. Variation of spectral index with flux in the shortest wavelength in FUV. The solid lines are the linear least squares fit to the data that take into account the errors in both α and fluxes, while the dashed lines are the un-weighted linear least squares fit to the data.

in AGN by Sakata *et al.* (2011), who also found a bluer when brighter trend in their sample. Similar conclusion was also arrived at by Wilhite *et al.* (2005) and Vanden Berk *et al.* (2004) in the optical band. Our results for a majority of the sources are also consistent with the observations of Paltani and Walter (1996) who found that the UV spectra of Seyfert galaxies becomes flatter with increased brightness of the sources. To explain these observations, Paltani and Walter (1996) proposed the two component model. According to this model, the observed flux is a superposition of two distinct spectral components, with constant spectral shapes. One component is flux variable while the other one is stable, and the observed continuum variation is driven by the amplitude of the varying component. For some sources in our sample such as NGC 3783, NGC 4151, NGC 4593 and Fairall 9, we in fact observed a constancy of the spectral index with increasing flux, however, only beyond

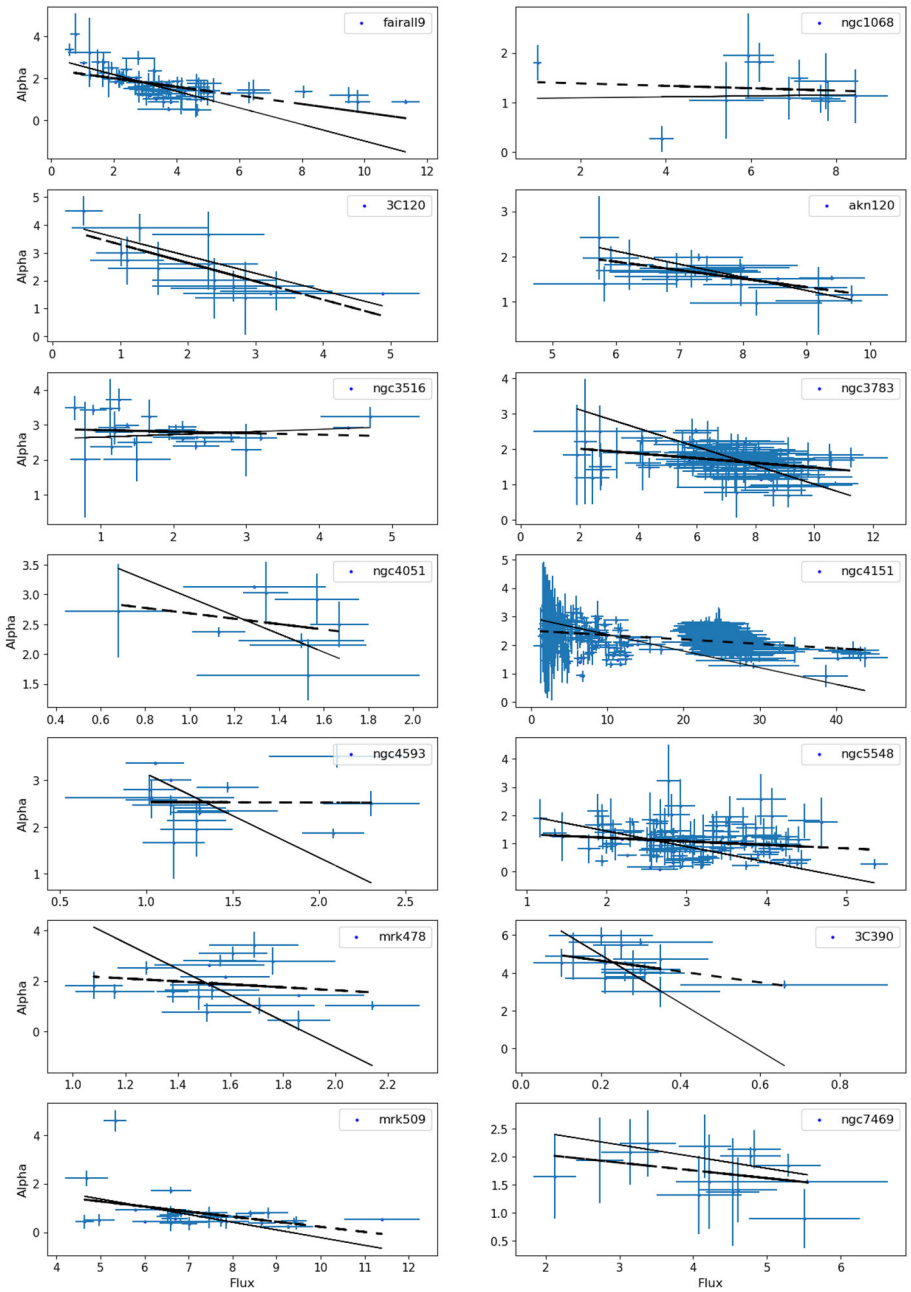

Figure 11. Variation of spectral index with flux in the NUV band. Linear least squares fit to the data that takes into account the errors in both the spectral indices and flux values are shown as solid lines. The un-weighted linear least squares fit to the data are shown with dashed lines.

certain flux levels in them. This points to the complex nature of UV flux variations in AGN (cf. Paltani & Walter 1996). The mean values of α for the sources in SWP and LWP are given in Table 2. Also, given in the same table are the mean α values reported by Paltani and Walter (1996) estimated using IUE spectra covering the wavelength range of 1150–3200 Å. For the sources that are in common between this study and that of Paltani and Walter (1996), the mean α values are similar, although the data analysed here is much more extensive than that of Paltani and Walter (1996).

5. Lag between different wavebands

To check for inter-band time lags we used the discrete correlation function (DCF) technique of Edelson and Krolik (1988). The cross-correlation analysis was done between the light curves of the shortest and longest

Table 4. Results of the linear least squares fit between the variation of spectral indices and the fluxes at the shortest wavelength in NUV and FUV bands. The columns r and P are the correlation coefficient and probability respectively.

	SWP				LWP			
Name	Slope	Intercept	*r*	*P*	Slope	Intercept	*r*	*P*
Fairall 9	-0.100 ± 0.012	1.425 ± 0.083	0.405	0.000	-0.393 ± 0.033	2.965 ± 0.105	0.601	0.000
NGC 1068	-0.065 ± 0.038	2.188 ± 0.353	0.530	0.052	0.009 ± 0.078	1.075 ± 0.489	−0.109	0.751
3C 120	-0.178 ± 0.038	2.268 ± 0.326	0.455	0.044	-0.622 ± 0.116	4.131 ± 0.345	0.760	0.002
Akn 120	-0.131 ± 0.026	3.097 ± 0.301	0.530	0.001	-0.291 ± 0.071	3.866 ± 0.556	0.653	0.001
NGC 3516	-0.079 ± 0.007	2.157 ± 0.036	0.286	0.008	0.074 ± 0.026	2.577 ± 0.098	−0.101	0.637
NGC 3783	-0.088 ± 0.006	2.204 ± 0.068	0.683	0.000	-0.262 ± 0.030	3.634 ± 0.217	0.329	0.000
NGC 4051	-1.140 ± 0.223	3.653 ± 0.326	0.596	0.001	-1.525 ± 0.873	4.472 ± 1.199	0.285	0.457
NGC 4151	-0.019 ± 0.001	1.310 ± 0.027	0.720	0.000	-0.058 ± 0.006	2.951 ± 0.090	0.380	0.000
NGC 4593	-0.002 ± 0.007	2.302 ± 0.018	0.378	0.043	-1.798 ± 0.626	4.939 ± 0.802	0.010	0.971
NGC 5548	-0.234 ± 0.019	2.280 ± 0.085	0.547	0.000	-0.547 ± 0.075	2.533 ± 0.250	0.179	0.050
Mrk 478	-1.201 ± 0.621	4.474 ± 1.896	0.181	0.518	-5.171 ± 2.293	9.716 ± 3.427	0.177	0.483
3C 390.3	-1.043 ± 0.142	2.160 ± 0.172	0.609	0.000	-12.695 ± 4.974	7.483 ± 1.222	0.445	0.084
Mrk 509	-0.038 ± 0.017	1.653 ± 0.191	0.097	0.485	-0.318 ± 0.098	2.956 ± 0.722	0.388	0.031
NGC 7469	-0.221 ± 0.009	2.982 ± 0.067	0.786	0.000	-0.211 ± 0.093	2.846 ± 0.460	0.360	0.206

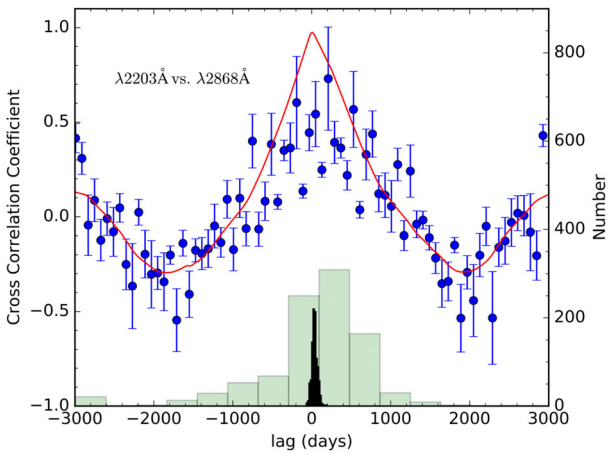

Figure 12. Cross-correlation analysis between the light curves at 2203 Å and 2868 Å for the source Fairall 9, one of the sources in the sample. The red solid line is for ICCF and the blue filled circles are for the DCF. The green and black histograms show the distribution of centroids for DCF and ICCF respectively.

wavelengths in both FUV and NUV for all the sources. We show in Fig. 12 the results on one correlation analysis for the object Fairall 9 carried out between the light curves at 2203 and 2868 Å. Here, the filled circles are those evaluated using the DCF method and the solid line is that obtained using the interpolated cross correlation function (ICCF) described in detail in Gaskell and Sparke (1986) and Gaskell and Peterson (1987). To evaluate the uncertainty in the derived lag, we followed a model of independent Monte Carlo approach that incorporated both flux randomization (FR) and random subset sampling (RSS) described in Peterson *et al.* (1998). For each Monte Carlo iteration, we found the lag using the centroid of the CCF utilizing all points within 60% of the peak of the CCF in the case of DCF. However, for ICCF the peak of the CCF was considered as a representation of the lag between the light curves. This was repeated for 10,000 times and the distribution of the CCF lags were obtained for both DCF and ICCF methods. The mean of the distributions were taken to represent the lag between the light curves and the spread in the distributions was used to estimate the error in the lag. The distributions obtained using both DCF (green histogram) and ICCF (black histogram) are given in Fig. 12 for the source Fairall 9. We found no noticeable time lag between flux variations in NUV and FUV bands, although the flux variations between different NUV and FUV bands were correlated. This analysis repeated for all the sources studied here yielded no measurable lags in any of them.

6. Conclusion

In the present work, we report the variability of fourteen Seyfert galaxies in the UV band using data from IUE acquired over a period of about 17 years. The flux values for the sources studied here in different NUV and FUV bands were taken from Dunn *et al.* (2006).

Various analysis were performed to characterise the flux variability of the sources. The summary of the work is given below:

1. All sources were found to show flux variations in the UV band. No statistically significant difference in the amplitude of flux variations between shorter and longer wavelengths was noticed.
2. No time lag between flux variations in different NUV and FUV bands was observed.
3. We found a mild negative correlation of variability with bolometric luminosity with high luminous sources showing low variability than their less luminous counterparts. Also, a hint for a positive correlation is found between variability and black hole mass. These results are consistent with what is known in literature.
4. Majority of source showed a bluer when brighter trend in the FUV data; however, such a trend, if any in NUV band is seen only in a minority of the sources that too moderately. Some sources showed a hardening of the spectrum with flux, but the spectrum remained non-variable beyond certain flux level. The observed spectral variations are thus complex.

Acknowledgements

We thank the anonymous referee for his/her critical comments that helped to improve the manuscript

References

Alloin D. *et al*. 1995, A&A, 293, 293A
Bentz M. C., Katz S. 2015, PASP, 127, 67
Bessel M. S. 1979, PASP, 91, 589
Cardelli J. A., Clayton G. C., Mathis J. S. 1989, ApJ, 345, 245
Dunn J. P., Jackson B., Deo R. P. *et al*. 2006, PASP, 118, 572
Edelson R. 1992, ApJ, 401, 516
Edelson R. A., Saken J., Pike G. *et al*. 1991, ApJL, 372, L9
Edelson R. A., Krolik J. H. 1988, ApJ, 333, 646
Elvis M. et al. 1994, APJ Supplement Series, 95, 1
Frank J., King A., Raine, D. J. 2002, in by Frank J., King A., Raine D., eds, Accretion Power in Astrophysics. Cambridge University Press, Cambridge, p. 398. ISBN 0521620538, February 2002
Gaskell C. M., Peterson B. M. 1987, ApJS, 65, 1
Gaskell C. M., Sparke L. S. 1986, ApJ, 305, 175
Giveon U., Maoz D., Kapsi S., Netzer H., Smith P. S. 1999, MNRAS, 306, 637
Greenhill L. J., Gwinn C. R. 1997, Ap&SS, 248, 261
Lohfink A. M., Reynolds C. S., Vasudevan R., Mushotzky R. F., Miller N. A. 2014, Apj, 788, 10
Lynden-Bell D. 1969, Nature, 223, 690
Meusinge H., Weiss V. 2013, A&A, 560, A104
Paltani S., Courvoisier T. J.-L. 1994, A&A, 291, 74
Paltani S., Walter R. 1996, A&A, 312, 55
Paltani S., Courvoisier T. 1997, A&A, 323, 717
Peterson B. M., Wanders I., Horne K., Collier S., Alexander T., Kaspi S., Maoz D. 1998. The Publication of the Astronomical Society of the Pacific, 110(748), 660
Rakshit S., Stalin C. S. 2017, ApJ, 842, 96
Rees M. J. 1984, ARAA, 22, 471
Rodriguez-Pascual *et al*., A&A, 72, 327
Sakata Y., Morokuma T., Minezaki T. *et al*. 2011, ApJ, 731, 50
Schlafly E. F., Finkbeiner D. P. 2011, ApJ, 737, 103
Stalin C. S., Gopal Krishna, Sagar R., Wiita P. J. 2004, Journal of Astrophysics and Astronomy, 25, 1
Ulrich M.-H., Maraschi L., Urry C. M. 1997, ARAA, 35, 445
Vanden Berk D. E., Wilhite B. C., Kron R. G., Anderson S. F., Brunner R. J., Hall P. B., Ivezić Ž., Richards G. T., Schneider D. P., York D. G. 2004, ApJ, 601, 692
Vaughan S., Edelson R., Warwick R. S., Uttley P. 2003, MNRAS, 345, 1271
Wagner S. J., Witzel A. 1995, ARAA, 33, 163
Wang X. Y., Dai Z. G., Lu, T. 2001 ApJ, 556, 1010
Welsh B. Y., Wheatley J. M., Neil J. D. 2011, A&A, 527, A15
Welsh W. F., Peterson B. M., Koratkar A. P., Korista K. T. 1998, ApJ, 509, 118
Wilhite B. C., Vanden Berk D. E., Kron R. G., Schneider D. P., Pereyra N., Brunner R. J., Richards G. T., Brinkmann J. V. 2005, ApJ, 633, 638
Wilhite B. C., Brunner R. J., Grier C. J., Schneider D. P., Vanden Berk D. E. 2008, MNRAS, 383, 1232
Wold M., Brotherton M. S., Shang Z. 2007, MNRAS, 375, 989
Zhang X.-G., Feng L. 2017, MNRAS, 464, 2203
Zuo W., Wu X.-B., Liu Y.-Q., Jiao C.-L. 2012, ApJ, 758, 104